processes

MDPI

Article

Simulation of the Adsorption Bed Process of Activated Carbon with Zinc Chloride from Spent Coffee Grounds for the Removal of Parabens in Treatment Plants

Wagner Vedovatti Martins [1], Adriele Rodrigues Dos Santos [2], Gideã Taques Tractz [3], Lucas Bonfim-Rocha [4], Ana Paula Peron [1,2,5] and Osvaldo Valarini Junior [1,2,*]

[1] Graduate Program in Technological Innovations, Federal Technological University of Paraná, Campo Mourão 87301-899, Paraná, Brazil; wagner.vedovatti@gmail.com (W.V.M.); anaperon@utfpr.edu.br (A.P.P.)
[2] Postgraduate Program in Food Technology (PPGTA), Federal Technological University of Paraná, Campo Mourão 87301-899, Paraná, Brazil; adrielesantos@utfpr.edu.br
[3] Academic Department of Chemistry (DAQUI), Federal Technological University of Paraná, Campo Mourão 87301-899, Paraná, Brazil; gideatractz@utfpr.edu.br
[4] Department of Chemical Engineering, Federal Technological University of Paraná, Londrina 86036-370, Paraná, Brazil; lucasrocha@utfpr.edu.br
[5] Graduate Program in Environmental Engineering, Federal Technological University of Paraná, Francisco Beltrão 85602-863, Paraná, Brazil
* Correspondence: osvaldovalarini@utfpr.edu.br; Tel.: +55-44-3518-1430

Abstract

Parabens—specifically methylparaben (MeP), ethylparaben (EtP), propylparaben (PrP), and butylparaben (BuP)—are widely used substances in everyday life, particularly as preservatives in pharmaceutical and food products. However, these compounds are not effectively removed by conventional water and wastewater treatment processes, potentially causing disruptions to human homeostasis and the endocrine system. This study conducted a transport and dimensional analysis through simulation of the adsorption process for these parabens, using zinc chloride-activated carbon derived from spent coffee grounds ($ACZnCl_2$) as the adsorbent, implemented via Aspen Properties® and Aspen Adsorption®. Simulations were performed for two inlet concentrations (50 mg/L and 100 mg/L) and two adsorption column heights (3 m and 4 m), considering a volumetric flow rate representative of a medium-sized city with approximately 100,000 inhabitants. The results showed that both density and surface tension of the parabens varied linearly with increasing temperature, and viscosity exhibited a marked reduction above 30 °C. Among the tested conditions, the configuration with 50 $mg \cdot L^{-1}$ inlet concentration and a 4 m column height demonstrated the highest adsorption capacity and better performance under adsorption–desorption equilibrium. These findings indicate that the implementation of adsorption beds on an industrial scale in water and wastewater treatment systems is both environmentally and socially viable.

Keywords: Aspen Plus® and Adsorption®; aliphatic parabens; water treatment; dynamic simulation; filtered coffee cake

check for updates

Academic Editors: Alejandro Regalado-Méndez, Reyna Natividad and Rubi Romero

Received: 4 July 2025
Revised: 23 July 2025
Accepted: 1 August 2025
Published: 6 August 2025

Citation: Martins, W.V.; Santos, A.R.D.; Tractz, G.T.; Bonfim-Rocha, L.; Peron, A.P.; Junior, O.V. Simulation of the Adsorption Bed Process of Activated Carbon with Zinc Chloride from Spent Coffee Grounds for the Removal of Parabens in Treatment Plants. *Processes* **2025**, *13*, 2481. https://doi.org/10.3390/pr13082481

Copyright: © 2025 by the authors. Licensee MDPI, Basel, Switzerland. This article is an open access article distributed under the terms and conditions of the Creative Commons Attribution (CC BY) license (https://creativecommons.org/licenses/by/4.0/).

1. Introduction

Lifestyle changes over the last decade have significantly altered human behavior. Parabens are synthetic chemical compounds widely used across various industrial sectors, including food products, preservatives, cosmetics, and pharmaceuticals [1]. The long-term

use of parabens has raised concerns about their potential impact on the human endocrine system and the possible disturbances they may cause to homeostasis [2,3]. Additionally, their association with hormonal disorders has also been increasingly investigated [4].

Parabens are composed of ester bonds linked to various functional groups, most commonly linear and open-chain alkyl radicals such as methylparaben (MeP), ethylparaben (EtP), propylparaben (PrP), and butylparaben (BuP) [5]. Their physicochemical properties vary depending on the attached radicals, with increasing alkyl chain length resulting in greater hydrophobicity. In their pure form, these compounds are white, solid, odorless, and have a mild burnt taste [4]. Parabens are water-soluble [1] and are found as residues in various matrices, including wastewater, surface water, drinking water, soil, sludge, urine, blood serum, seminal plasma, tissues, and mammary placentas [6]. In Brazil, the reported concentrations range as follows: MeP-0.11–0.98 μg/L, EtP 0.38–9.70 μg/L, PrP-0.70–7.90 μg/L, and BuP-1.90–11.0 μg/L [6,7].

Several treatment methods have been proposed, including microextraction [8] and sorptive extraction [9]. However, due to the limited data on the presence of parabens in various environmental matrices, especially in developing countries such as Brazil and different regions in Africa [10], no regulatory limits have yet been established. This highlights the urgent need to simulate non-conventional treatment processes for these chemical compounds. The absence of regulation could lead to a progressive accumulation of parabens in the aforementioned environments.

Conventional water and wastewater treatment methods are currently ineffective in removing such organic contaminants. Therefore, alternative unit processes such as advanced oxidation processes, membrane separation, heterogeneous photocatalysis, electroprecipitation, and adsorption are gaining interest for the removal of organic pollutants [11]. Among these alternatives, adsorption stands out as one of the most promising due to its advantages: low sludge generation, use of low-cost and abundant reagents, potential for circular economy applications, high removal efficiency, and practical feasibility for both industrial and environmental applications [3,12,13].

Materials with circular economy potential—particularly those rich in carbon chains—are suitable for chemical modification and impregnation with reactive agents for the adsorption of parabens. Among various agricultural residues, such as rice husks and clay, spent coffee grounds (from *Coffea arabica*) are a promising raw material for producing activated carbon (AC) [14]. Coffee waste is generated from a globally significant commodity, producing millions of sacks annually [15], with approximately 2.1 billion tons of spent coffee grounds being discarded each year [16]. This biomass, which contains approximately 50% carbon, is currently sent to landfills despite its environmental toxicity. When converted into AC, especially using chemical activating agents such as zinc chloride ($ZnCl_2$), the resulting material exhibits enhanced internal porosity, a microcrystalline structure, and microporous surface areas, along with good selectivity for adsorption. It can also form various surface functional groups, including carboxylic acids, hydroxyls, lactone carbonyls, and quinones [17,18].

In the context of paraben removal, optimizing the adsorption process plays a critical role in the potential implementation of this technology in water and wastewater treatment facilities. Computational tools such as Aspen Plus® and Aspen Adsorption® are essential for applications in chemical, environmental, sanitary, and energy engineering. Aspen Plus® allows the modeling of transport and thermodynamic properties across various unit operations, including chemical reactors, heat exchangers, and separation systems. Aspen Adsorption® enables manipulation of process variables that affect adsorption, such as kinetic constants and mass transfer coefficients [19].

Given the scarcity of studies focused on analyzing adsorption at an industrial scale and the pressing need for treating paraben-contaminated aquatic environments, this study aims to evaluate the adsorption capacity of $ZnCl_2$-activated carbon ($ACZnCl_2$) for the removal of MeP, EtP, PrP, and BuP. This will be accomplished using component property data (Aspen Properties) and breakthrough curves simulated using a proposed model implemented in Aspen Adsorption® V14.

2. Materials and Methods

2.1. Experimental Information

The physical properties of $ZnCl_2$-activated carbon ($ACZnCl_2$) were obtained from previous studies conducted by the research group using this adsorbent [11,18]. The $ACZnCl_2$ was synthesized using spent coffee grounds, a material primarily composed of carbonaceous and lignocellulosic matter. The synthesis involved treating the spent coffee grounds with $ZnCl_2$ at a 2:1 ratio (spent coffee grounds: chemical reagent). This mixture was held at 85 °C for 7 h, after which the temperature was increased to 110 °C for 24 h. Following the material's cooling and moisture stabilization, the sample underwent calcination in a Coel muffle furnace (Manaus, Brazil). This calcination was performed at 600 °C for 2 h under an inert nitrogen atmosphere, maintained at a flow rate of approximately 1 mL/min. Finally, the activated carbon was purified by washing it with 0.1 M HCl for 20 min, followed by a wash with deionized water at 85 °C for 20 min. The material was then sieved at 25 °C using 100-mesh sieves to standardize its particle size. The spent coffee grounds were supplied by COAMO (Campo Mourão, Brazil) [11,20]. It applied Aspen Propriety® V14 to simulate the propriety of the transport, and Aspen Adsorption® V14 to simulate the fixed-bed column adsorption process. The experimental values used in the simulations are presented in Table 1.

Table 1. Physicochemical properties of adsorbents and adsorbates.

Property	Value	References
Concentration paraben—mg/L	50 and 100	Variable
Concentration water—kmol/m^3	55.55	Fixed
Height of adsorbent layer—(H_b) m	3 and 4	Variable
Particle radius—(R_P) m	8.47×10^{-8}	Fixed
Pore radius—(r_p) m	1.11×10^{-9}	Fixed
Diameter of adsorbent layer—(d_p) m	1.69×10^{-7}	Fixed
Inter-particle voidage—(ε_b) m^3·void/m^3·bed	0.50	Fixed
Particle porosity—ε_P	0.42	Fixed
Bulk density $-(p_{ACZnCl_2})$ kg/m^3	740	Fixed

2.2. Physicochemical Properties of Parabens

Aspen Properties® V14, a tool within the Aspen® platform, was used to obtain the physicochemical properties of pure parabens and their binary systems with water. The Non-Random Two-Liquid (NRTL) activity coefficient model was applied to estimate the thermodynamic properties of methylparaben (MeP), ethylparaben (EtP), propylparaben (PrP), and butylparaben (BuP) [21,22]. The physicochemical properties and molecular structures of the parabens used in this study were based on the data reported by Nowak et al. [1].

2.3. Simulations in Aspen Adsorption®

The adsorption process simulations for MeP, EtP, PrP, and BuP onto $ZnCl_2$-activated carbon ($ACZnCl_2$) were conducted based on the determination of key process parameters.

The molecular sizes of MeP, EtP, PrP, and BuP are considered smaller than the pore sizes of the $ACZnCl_2$ adsorbent; therefore, Knudsen diffusion was taken into account. The flow through the adsorption bed was assumed to occur only in the axial direction. The fixed-bed column was modeled with a uniform cross-sectional flow, operating under isothermal conditions without pressure drop and constant at the 1 bar. A constant linear velocity was assumed, and the adsorbent particles were considered to be spherical, uniform in size and density [21]. For the fixed-bed model, the Upwind 1 finite difference scheme was used for discretization.

2.3.1. Mass/Momentum Balance

In this study, the mass/momentum balance was formulated considering convective transport with estimated dispersion. The partial mass balance of parabens in a differential volume element of the column is described by the following partial differential equation (Equation (1)):

$$-\varepsilon_b \times D_z \times \frac{\partial^2 C}{\partial z^2} + \frac{\partial (v_i C)}{\partial z} + \varepsilon_b \times \frac{\partial C}{\partial t} + p_a \times \frac{\partial q}{\partial t} = 0 \quad (1)$$

Equation (1) includes the axial dispersion phenomena, 1st term, the mass transfer by convection, 2nd term, which means the accumulation of pollutant in adsorbents, the 3rd term, and the relationship that occurs by the adsorption process of MeP, EtP, PrP, BuP in adsorbent particles, D_z is the axial dispersion coefficient given in m^2/s, q is the concentration of parabens adsorbed in the solid phase mg/g, C is the concentration in the liquid phase in mg/L, z is the distance along the bed given in meters (m), v_i is the interstitial velocity of the fluid through the bed in m/s, ε_b is the void fraction of the bed, dimensionless, and p_a is the apparent density of the bed, kg/m^3, and D_z was estimated from Equation (2).

$$\frac{v_i \times d_P}{D_z} = 0.2 + 0.011 \times \left(\frac{Re}{\varepsilon_b}\right)^{0.48} \quad (2)$$

where d_p is the particle diameter of the adsorbent given in meters (m), Re is the Reynolds number used to determine whether the system is laminar or turbulent.

2.3.2. Kinetic Model

The kinetic model used in this study was the concentrated linear resistance model, specifically a first-order model. This model indicates that the mass transfer coefficient (K_i) occurs in the solid phase at a rate of s^{-1} and is represented by Equation (3).

$$\frac{\partial q}{\partial t} = K_i \times (q_e - q) \quad (3)$$

The variable q_e is defined as the instantaneous equilibrium capacity in mg/g. If we consider the resistance of the external fluid film and the diffusional resistance of the pores, K_i can be estimated by Equation (4).

$$\frac{1}{K_i} = \frac{R_P}{3 \times k_{fi}} + \frac{R_P^2}{15 \times \varepsilon_p \times D_P} \quad (4)$$

where k_{fi} is the mass transfer coefficient of the external film of adsorbate i, m^2/s, and D_p is the effective diffusivity coefficient of the pores, given in m^2/s. The missing parameters: k_{fi}, D_p, and the Knudsen diffusion coefficient D_k in m^2/s, as well as the molecular diffusion

coefficient of $ACZnCl_2$, Dm in m^2/s, were estimated using empirical correlations. The effective pore diffusivity coefficient (D_p) was estimated using the following correlation [23].

$$\frac{1}{D_p} = \tau_p \times \left(\frac{1}{D_m} + \frac{1}{D_k}\right) \tag{5}$$

The molecular diffusion coefficient (D_m) was estimated using the following correlation for nonelectrolytes in an infinitely dilute solution [21].

$$D_m = 7.4 \times 10^{-8} \times \frac{(\alpha_A \times M_s)^{0.5} \times T}{\eta_s \times V_m^{0.6}} \tag{6}$$

In Equation (6), (D_m) is in cm^2/s, Ms is molecular weight of solvent give in g/mol, T is temperature (K), η_s is the dynamic viscosity of solvent in kg/m·s, α_A is the association factor of solvent, and V_m is obtained from the Aspen Property at 298.15 K. Values are shown in Table S1. The Knudsen diffusion coefficient (D_k) and the tortuosity factor (τ_p) were estimated by Equations (7) and (8), respectively [23].

$$D_k = 97 \times \tau_p \times \left(\frac{T}{M_s}\right)^{0.5} \tag{7}$$

$$\tau_p = \varepsilon_p + 1.5 \times (1 - \varepsilon_p) \tag{8}$$

The external film mass transfer coefficient (k_{fi}) was calculated using Equation (9) [21].

$$Sh = \frac{k_{fi} d_p}{D_m} = 2 + 1.58 Re^{0.4} Sc^{1/3} \tag{9}$$

where Reynolds number and Schmidt number are estimated by Equations (10) and (11), respectively.

$$Sc = \frac{\eta_{sol}}{\rho_{sol} \times D_m} \tag{10}$$

$$Re = \frac{\rho_{sol} \times d_P \times v_s}{\eta_{sol}} \tag{11}$$

2.3.3. Adsorption Isotherm

The equilibrium isotherm used in this adsorption process of $ACZnCl_2$ with each paraben, MeP, EtP, PrP, and BuP, was the Langmuir model, which has been validated in many works of the group [11,18], and was a determinant of adsorption capacity, proportional maximum adsorption capacity, equilibrium concentration, and adsorption energy constant, and inversely proportional to one plus the equilibrium concentration times the maximum energy constant.

In Aspen Adsorption®, to use the Langmuir isotherm, the equilibrium adsorption capacity was replaced by w_i, which denotes the amount of solute adsorbed per unit mass of the adsorbent, changing the unit from mg/g to kmol/kg, the maximum adsorption capacity was expressed by IP_1, which represents the maximum adsorption capacity of the solid phase in a monolayer, in the same unit used for determination in modeling experimental equilibrium processes, and the adsorption energy constant is replaced by IP_2, changing the unit from L/mg to m^3/kmol. Thus, the Langmuir model for use in Aspen Adsorption is expressed by Equation (12).

$$w_i = \frac{IP_1 \times IP_2 \times C}{1 + IP_2 \times C} \tag{12}$$

The quantitative values for IP_1 and IP_2 can be calculated using Equation (13), where M represents the molar mass of the parabens in g/mol. The k_L and q_{max} parameters used in the simulations were obtained from studies employing a paraben concentration of 10 mg/L. For MeP and PrP, the reported q_{max} values are 167 and 151 mg/g, and the k_L values are 5.40 and 22.3 L/g, respectively [24]. Due to the lack of specific data, EtP was modeled using the same constants as MeP. For BuP, the values of q_{max} and k_L used were 7.52 mg/g and 0.093 L/g, respectively [17].

$$IP_1 = \frac{q_{max}}{1000 \times M} \rightarrow IP_2 = 1000 \times k_L \times M \quad (13)$$

The bed height (H_b), given in meters, is fixed. In the product section, the flow rate, temperature, and pressure remain constant, matching the values at the inlet of the adsorption process.

2.3.4. Column Performance Study

The analysis of the adsorption process for MeP, EtP, PrP, and BuP occurred according to the column rupture time t_{break} (min), volumetric flow rate (Q) m^3/min, saturation time t_{sat} (min), and total treated volume V_{eff} (m^3), estimated via Equations (14)–(16).

$$V_{eff} = Q \times t_{sat} \quad (14)$$

$$q_{max} = Q \times \int_{t=0}^{t=t_{sat}} C_R dt \quad (15)$$

$$q_e = \frac{q_{max}}{m} \quad (16)$$

The values were established within a range of 0.05 and 0.9 of $C \cdot C_i^{-1}$, where C_R is the concentration of MeP, EtP, PrP, and BuP adsorbed ($C \cdot C_i^{-1}$) mg/L, and m represents the mass of adsorbent used in the column in g.

3. Results and Discussion

3.1. Physical and Chemical Properties of Parabens

Figure 1 illustrates key properties that play a critical role in the transport of emerging pollutants during an adsorption process. It can be observed that, for all four parabens analyzed in this study, these properties decrease with increasing temperature.

Figure 1a presents the relationship between fluid density and temperature. The observed decrease in density is attributed to the gain in kinetic energy by the molecules, which results in increased intermolecular spacing. This leads to a reduction in fluid mass per unit volume. Consequently, lower density results in reduced hydrostatic pressure, which may enhance the penetration of the liquid phase into the pores of $ACZnCl_2$ [21].

Figure 1b shows that surface tension decreases as temperature increases. This occurs because molecules with higher kinetic energy experience weaker cohesive forces, making the solution more deformable and improving its ability to enter both macro- and micropores. Surface tension also affects the formation of liquid films on the adsorbent surface, thereby facilitating contact between adsorbent and adsorbate [25]. Figure 1c indicates that the viscosity of parabens decreases with increasing temperature. This reduction is due to the enhanced molecular motion, which overcomes intermolecular forces more easily. In the context of adsorption as a unit operation, lower viscosity promotes mass transfer by facilitating diffusion and penetration of the pollutant into the micropores of the $ACZnCl_2$ surface [26].

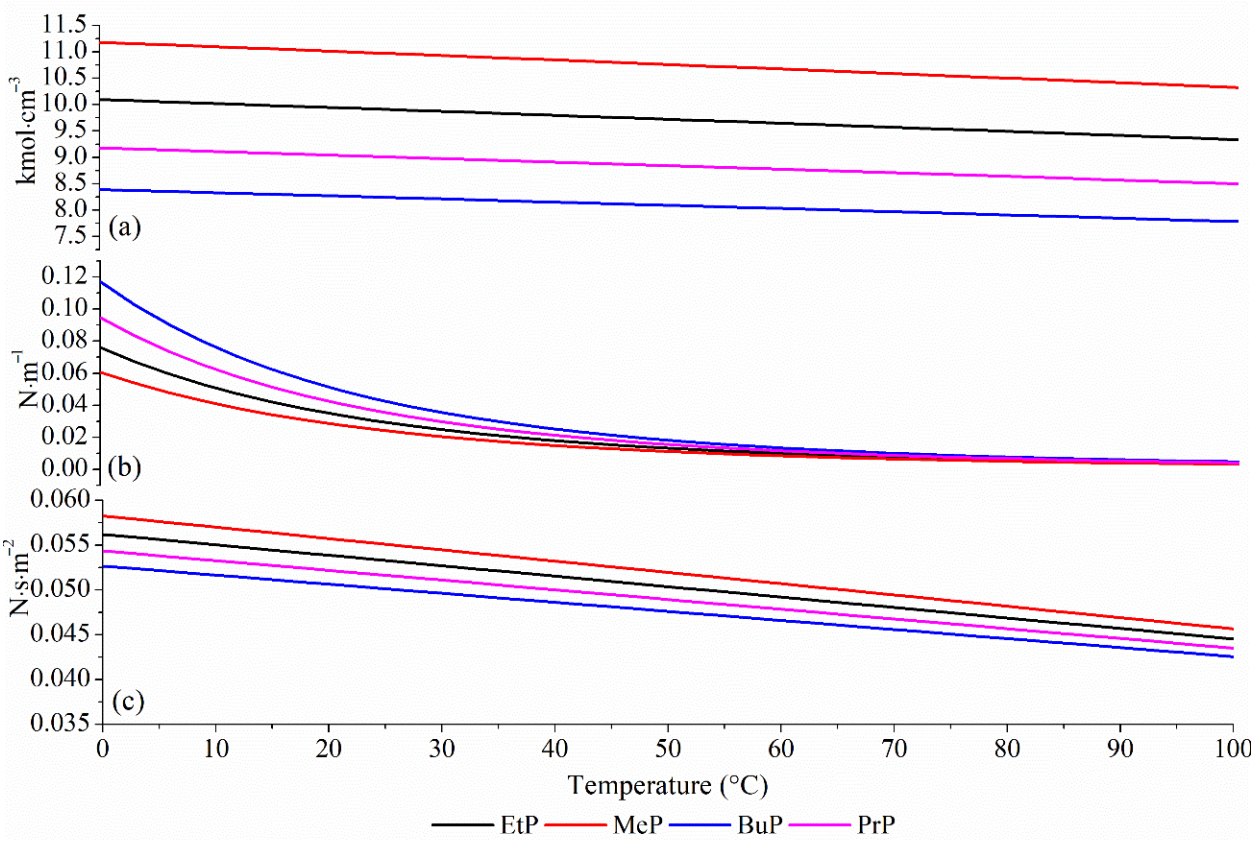


Figure 1. Analysis of pure compounds for density (**a**), surface tension (**b**), and viscosity (**c**).

3.2. Adsorption Column Simulation

Table 1 presents the fixed variables and system properties used and calculated for the adsorption column simulation. The paraben concentrations were intentionally set at values significantly higher than those currently reported in water bodies [6,7], based on the assumption that, due to the absence of regulatory standards, the environmental levels of these pollutants may increase exponentially soon. The average volumetric flow rate considered for sizing the adsorption column—assuming integration with a water or wastewater treatment plant—was 12,000 m^3/day [27,28].

Additional parameters used in the calculations are presented in Table 2 and were obtained by solving Equations (2)–(14). The water properties adopted in this study include the following: η_s, the dynamic viscosity of the solvent, 0.001 kg/m·s; α_A, the solvent association factor, 2.26; and the molar mass of water, 18.01 g/mol [21]. The bed height (H_b) values used as design parameters were 3 m and 4 m [25], and the column diameter was defined using the ratio $H_b/D = 10$ [29]. The Reynolds numbers (Re) obtained for each H_b were 0.33 for 3 m and 0.19 for 4 m, indicating that higher column heights result in lower interstitial fluid velocities. Additionally, increasing H_b can lead to a higher pressure drop. Conversely, shorter columns exhibit higher axial dispersion coefficients (D_z), which were found to be 5.82×10^{-7} m^2/s, 1.47×10^{-7} m^2/s, and 3.71×10^{-8} m^2/s for 3 m and 4 m, respectively. The values of the intraparticle diffusion coefficient (K_i) and molecular diffusivity in water (D_p) used were 2.7×10^{-3} m^2/s [30] and 5.1×10^{-11} m^2/s [31], respectively.

Table 2. Parameters calculated and utilized for a volumetric flow rate of 12,000 m^3/day using $ACZnCl_2$.

Parameters-Unit	MeP	EtP	PrP	BuP
Sc	0.0119	0.0112	0.0106	0.0101
D_m-m^2/s	8.41×10^{-5}	8.94×10^{-5}	9.47×10^{-5}	9.97×10^{-5}
D_k-m^2/s	4.37×10^{-7}			
D_p-m^2/s	3.37×10^{-7}	3.37×10^{-7}	3.37×10^{-7}	3.38×10^{-7}
K_i-s^{-1}	1.48×10^{8}			
IP_1-mmol/g	1.10×10^{-3}	1.00×10^{-3}	8.38×10^{-4}	3.87×10^{-5}
IP_2-L/mol	8.22×10^{5}	8.97×10^{5}	4.02×10^{6}	1.81×10^{4}

Table 2 presents the calculated parameters for all parabens evaluated in this work. It was observed that, as the molecular chain length of the parabens increases, all related parameters also increase. The bed height (H_b) did not significantly affect the equilibrium or kinetic constants. Finally, the IP_1 and IP_2 parameters of the Langmuir equilibrium isotherm, calculated from Equation (13), are also presented in Table 2. The initial simulation performed in this study aimed to evaluate the influence of column height on the outlet concentration of the contaminants. It was found that H_b directly affects the effluent concentration.

Based on the data in Table 2, Aspen Adsorption® was inserted into the treatment model analyzed (Figure 2).

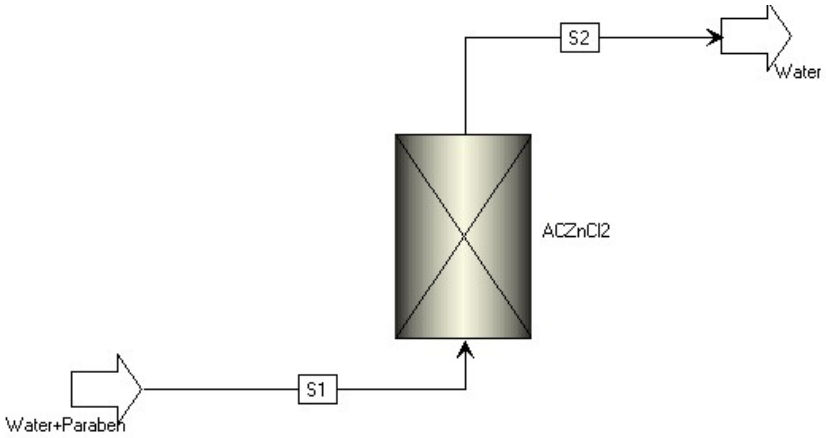


Figure 2. Flowsheet after conventional water and effluent treatment.

This type of treatment would be installed after conventional water and effluent treatment, since parabens can react with other ions and reagents present in the water or effluent during treatment, forming transformation products that can be more persistent or toxic than the original compounds. In conventional water treatment processes, adsorption with $ACZnCl_2$ should be implemented as a tertiary treatment step, following the primary (physical screening, sand removal, and primary clarification) and secondary (biological treatment, such as activated sludge, followed by secondary clarification) processes. At this stage, most of the organic matter, suspended solids, and nitrogen/phosphorus compounds have already been removed, significantly reducing the load on the activated carbon. This optimizes the efficiency and economic viability of the adsorption process for micropollutants such as parabens [32–34].

In wastewater treatment, the goal is to meet discharge limits and protect receiving water bodies. Wastewater contains a much larger and more diverse range of pollutants than raw water for potable use, including high organic loads, suspended solids, and various micropollutants. Therefore, pretreatment is crucial: Adequate pretreatment (e.g., coagulation, flocculation, sedimentation, filtration, biological treatment) is essential to remove

suspended solids, colloids, natural organic matter (NOM), and other macropollutants. These substances can contaminate the activated carbon bed, reducing its available surface area for paraben adsorption, increasing pressure drop, and requiring more frequent backwashing or regeneration [35–37].

The importance of adsorbent placement, empty bed contact time (EBT), regeneration, pressure drop, and chemical interactions is extremely important for the process as a whole. Failure to place them in the correct locations can result in the following: halogenation is a transformation product that can be generated by the reaction with chlorine (Cl_2), in systems with residual chlorine, such as in the disinfection of sewage or drinking water, reacting with the phenolic group of parabens, generating mono- and dichlorinated parabens. This alters the rate constants, which are dependent on pH, temperature, and the concentration of NH_4^+ (ammonium ion), leading to the formation of 3-chloro- and 3,5-dichloro-parabens [38,39]. Another transformation product that can be generated is oxidation with ozone (O_3), pure O_3 reacts slowly with undissociated parabens ~10^5 $M^{-1}{\cdot}s^{-1}$, and, at high pH, it forms OH^- radicals on a scale in ~10^9 $M^{-1}{\cdot}s^{-1}$ [40]. From the data entered into the software, the following paraben fractions were obtained as a function of time (Figure 3).

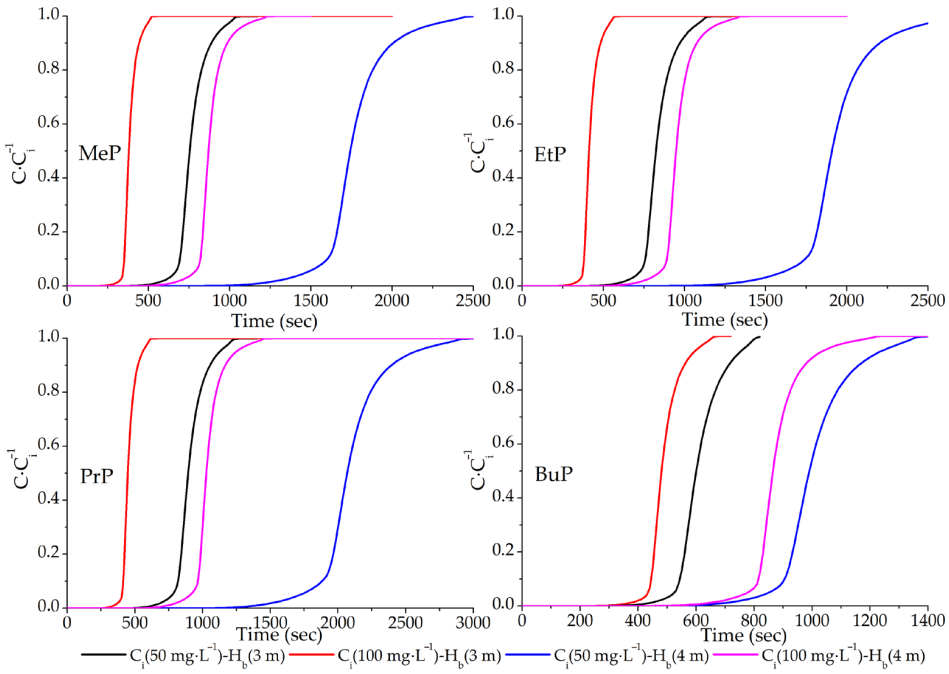


Figure 3. Adsorption advancement curves of parabens in $ACZnCl_2$ by varying bed height and concentration.

Figure 3 presents the time-dependent analysis of the adsorption process for the four tested parabens using $ACZnCl_2$ as the adsorbent, at initial concentrations of 50 and 100 mg/L and bed heights of 3 and 4 m, respectively. When analyzing each paraben individually, a consistent trend was observed: systems with an initial concentration of 100 mg/L exhibited an earlier breakthrough time (t_{break}) compared to those with an initial concentration of 50 mg/L. Furthermore, the data show that shorter bed heights (H_b) led to faster saturation times (t_{sat}). This behavior can be attributed to several factors, including the compound's polarity, operational pH, temperature, and, most notably, the specific surface area of the adsorbent [11]. In adsorption processes, the fastest adsorption typically occurs within the interior of the pores, driven by intraparticle diffusion and concentration gradients of the adsorbate [12]. The adsorption–desorption capacity in this study is phenomenologically correlated with the initial concentration (C_i) in the first-order kinetic

model. Systems with higher C_i values generally exhibit faster adsorption onto active sites compared to those with lower initial concentrations [11,20].

Another key feature observable in Figure 3 is the mass transfer zone (MTZ), defined as the interval between the breakthrough time (t_{break}) and the saturation time (t_{sat}). This region of the adsorption front progresses along the bed and over time. An exponential increase in this zone was observed, likely due to the presence of unsaturated pores within the $ACZnCl_2$ structure in this region [11,18,20]. The width of the MTZ reflects the efficiency of bed utilization: the narrower the zone, the more efficient the adsorption process [12]. The saturation time (t_{sat}) marks the maximum operational limit of the system, indicating the point at which the active sites in the $ACZnCl_2$ pores become fully occupied. Beyond this point, the adsorption–desorption equilibrium becomes dominant and constant on the adsorbent surface. This stage, governed by molecular diffusion from the aqueous solution to the adsorbent surface, is relatively slow and precedes the need for adsorbent regeneration or replacement [12]. Table 3 shows the performance calculations of the columns analyzed in this study.

Table 3. Column parameters obtained at various inlet concentrations and bed heights.

Parabens	C_i mg/L	H_b m	t_{break} min	t_{sat} min	V_{eff} m^3	q_{max} mg	q_e mg/g
MeP	50	3	8.6	16.6	0.0387	3.869	0.77
	100	3	5.2	8.8	0.0206	2.057	0.41
	50	4	18.2	41.5	0.0968	9.683	1.94
	100	4	10.5	20.5	0.0478	4.783	0.96
EtP	50	3	9.5	25.5	0.0595	5.950	1.19
	100	3	5.3	12.9	0.0301	3.006	0.60
	50	4	10.2	40.2	0.0937	9.372	1.87
	100	4	10.8	22.5	0.0525	5.250	1.05
PrP	50	3	8.3	20.8	0.0486	4.861	0.97
	100	3	4.7	10.4	0.0242	2.419	0.48
	50	4	19.2	47.7	0.1112	11.122	2.22
	100	4	10.1	24.2	0.0564	5.639	1.13
BuP	50	3	7.1	13.6	0.0318	3.181	0.64
	100	3	5.9	10.8	0.0253	2.528	0.51
	50	4	10.9	22.8	0.0533	5.328	1.07
	100	4	10.2	20.7	0.0482	4.822	0.96

Based on Figure 3, the breakthrough time (t_{break}) and saturation time (t_{sat}) were analyzed for different bed height (H_b) configurations and paraben concentrations. Equations (14)–(16) were applied using an adsorbent concentration of 5 g/L [2] and a flow rate of 12,000 m^3/day to calculate the unknown parameters presented in Table 3. All time units were converted to minutes. Under the assumption of constant interstitial velocity, it was observed that H_b significantly influences both t_{break} and t_{sat} in fixed-bed adsorption columns. For all four parabens tested—MeP, EtP, PrP, and BuP—it is evident that shorter columns lead to faster bed saturation and reduced mass transfer zone (MTZ) width [21,25]. When analyzing the influence of concentration alone, it was also noted that lower inlet concentrations resulted in higher maximum adsorption capacities (q_{max}). This outcome is attributed to two factors. First, higher concentrations initiate adsorption more rapidly due to the greater driving force [11,20]. Second, shorter residence times in the column limit the opportunity for the paraben molecules to diffuse into the mesopores and micropores of the $ACZnCl_2$, thereby reducing deposition in the internal structure of the adsorbent [21].

From a process design perspective, the optimal configuration must balance residence time so that it is neither excessively long nor too short, while still allowing equilibrium to be reached within the system. This ensures that the adsorption step does not become a limiting factor in full-scale water or wastewater treatment processes. As shown in Table 3, shorter saturation times correspond to lower q_{max} values [41]. Although simulation studies involving paraben adsorption are unprecedented, similar behaviors have been reported in other adsorption modeling studies for organic pollutants [21,42]. Ultimately, considering all results, the most effective configuration identified in this study—consistent across all parabens tested—is an inlet concentration of 50 mg/L combined with a bed height of 4 m, which provided the highest q_{max} and q_e values for the designed systems.

Future research focuses on monitoring and control, as continuous monitoring of paraben concentrations in the adsorption bed effluent is essential for detecting when parabens begin to appear in the treated water, signaling that the bed is approaching saturation and requires regeneration or replacement. A thorough assessment of pressure drop and monitoring of this variable in the bed indicates potential clogging due to particle or biomass growth, requiring backwashing. The cost–benefit analysis of implementing these processes, including the capital cost of installing the adsorption columns, operational costs, and maintenance, must be weighed against the benefits of paraben removal and public health protection. Finally, a pilot plant study of the entire treatment process to remove parabens is needed to validate the designed and simulated parameters.

4. Conclusions

This study evaluated the technical feasibility of implementing a paraben treatment system in water and wastewater treatment plants based on dynamic simulation results of the adsorption of MeP, EtP, PrP, and BuP in a fixed-bed column packed with $ACZnCl_2$. An industrial-scale adsorption column was proposed to assess the adsorption capacity of parabens in contaminated drinking water for individual domestic use. Based on the optimized simulation results, the industrial-scale adsorption column is shown to be suitable for individual domestic applications. To treat drinking water contaminated with 50 $mg \cdot L^{-1}$ of parabens under daily usage conditions, the column should be designed with a height-to-diameter ratio (H_B/D) of 10, a bed height of 3 m, and $ACZnCl_2$ particle diameters of 1.69×10^{-7} m. The system operates with an inlet liquid flow rate of 12,000 m^3/day. Under these conditions, the fixed-bed column can supply treated water continuously, requiring complete bed replacement once per day, as the activated carbon may reach saturation at a breakthrough concentration ratio ($C \cdot C_i^{-1}$) of up to 0.999. Finally, it is essential to emphasize the importance of treating wastewater and contaminated water containing emerging pollutants, such as parabens, as a means of ensuring sanitary safety and minimizing the occurrence of health issues related to homeostatic imbalances and endocrine disorders in local populations.

Supplementary Materials: The following supporting information can be downloaded at: https://www.mdpi.com/article/10.3390/pr13082481/s1, Table S1. Parameters utilized for a volumetric flow rate of 12,000 m^3/day using $ACZnCl_2$.

Author Contributions: Conceptualization, O.V.J. and A.P.P., methodology, W.V.M., A.R.D.S. and G.T.T.; writing—original draft preparation, O.V.J. and L.B.-R.; writing—review and editing, O.V.J. All authors have read and agreed to the published version of the manuscript.

Funding: This research received no external funding.

Data Availability Statement: The original contributions presented in this study are included in the article/Supplementary Materials. Further inquiries can be directed to the corresponding author.

Acknowledgments: Each of the authors made original contributions to this article; questions can be directed to the corresponding author.

Conflicts of Interest: The authors declare no conflicts of interest.

References

1. Nowak, K.; Ratajczak-Wrona, W.; Górska, M.; Jabłońska, E. Parabens and Their Effects on the Endocrine System. *Mol. Cell. Endocrinol.* **2018**, *474*, 238–251. [CrossRef]
2. Tsubouchi, L.M.S.; de Almeida, E.A.; Santo, D.E.; Bona, E.; Pereira, G.L.D.; Jegatheesan, V.; Cardozo-Filho, L.; Peron, A.P.; Junior, O.V. Production and Characterization of Graphene Oxide for Adsorption Analysis of the Emerging Pollutant Butylparaben. *Water* **2024**, *16*, 3703. [CrossRef]
3. Correa-Navarro, Y.M.; Rivera-Giraldo, J.D.; Cardona-Castaño, J.A. Modified Cellulose for Adsorption of Methylparaben and Butylparaben from an Aqueous Solution. *ACS Omega* **2024**, *9*, 30224–30233. [CrossRef]
4. Giulivo, M.; Lopez de Alda, M.; Capri, E.; Barceló, D. Human Exposure to Endocrine Disrupting Compounds: Their Role in Reproductive Systems, Metabolic Syndrome and Breast Cancer. A Review. *Environ. Res.* **2016**, *151*, 251–264. [CrossRef]
5. Boberg, J.; Taxvig, C.; Christiansen, S.; Hass, U. Possible Endocrine Disrupting Effects of Parabens and Their Metabolites. *Reprod. Toxicol.* **2010**, *30*, 301–312. [CrossRef]
6. Chen, M.H.; Yu, B.; Zhang, Z.F.; Ma, W.L. Occurrence of Parabens in Outdoor Environments: Implications for Human Exposure Assessment. *Environ. Pollut.* **2021**, *282*, 117058. [CrossRef] [PubMed]
7. Derisso, C.R.; Pompei, C.M.E.; Spadoto, M.; da Silva Pinto, T.; Vieira, E.M. Occurrence of Parabens in Surface Water, Wastewater Treatment Plant in Southeast of Brazil and Assessment of Their Environmental Risk. *Water Air Soil Pollut.* **2020**, *231*, 231–468. [CrossRef]
8. Ariffin, M.M.; Azmi, A.H.M.; Saleh, N.M.; Mohamad, S.; Rozi, S.K.M. Surfactant Functionalisation of Magnetic Nanoparticles: A Greener Method for Parabens Determination in Water Samples by Using Magnetic Solid Phase Extraction. *Microchem. J.* **2019**, *147*, 930–940. [CrossRef]
9. Han, J.H.; Cui, Y.Y.; Yang, C.X. Tailored Amino/Hydroxyl Bifunctional Microporous Organic Network for Efficient Stir Bar Sorptive Extraction of Parabens and Flavors from Cosmetic and Food Samples. *J. Chromatogr. A* **2021**, *1655*, 462521. [CrossRef]
10. Bolujoko, N.B.; Unuabonah, E.I.; Alfred, M.O.; Ogunlaja, A.; Ogunlaja, O.O.; Omorogie, M.O.; Olukanni, O.D. Toxicity and Removal of Parabens from Water: A Critical Review. *Sci. Total Environ.* **2021**, *792*, 148092. [CrossRef]
11. Rocha, B.C.d.S.; de Moraes, L.E.Z.; Santo, D.E.; Peron, A.P.; Souza, D.C.d.; Bona, E.; Valarini, O. Removal of Bentazone Using Activated Carbon from Spent Coffee Grounds. *J. Chem. Technol. Biotechnol.* **2024**, *99*, 1342–1355. [CrossRef]
12. do Nascimento, R.F.; de Lima, A.C.A.; Vidal, C.B.; Melo, D.d.Q.; Raulino, G.S.C. *Adsorção: Aspectos Teóricos e Aplicações Ambientais*; Fortaleza Imprensa Universitária: Fortaleza, Brazil, 2020; p. 308.
13. Ribas, F.B.T.; da Silva, W.L. Biosorption: A Review of Promising Alternative Methods in Wastewater Treatment. *Rev. Mater.* **2022**, *27*, e13212. [CrossRef]
14. dos Santos Gonçalves Nascimento, G.C.; da Cunha Barros, D.G.; Ratuchinski, L.S.; Okon, C.; Bressiani, P.A.; Santo, D.E.; Duarte, C.C.S.; Ferreira, P.M.P.; Junior, O.V.; Pokrywiecki, J.C.; et al. Adverse Effects of Octocrylene on Cultivated and Spontaneous Plants and in Soil Animal. *Water Air Soil Pollut.* **2023**, *234*, 109688. [CrossRef]
15. Siregar, C.A.; Siregar, A.M.; Lubis, R.W.; Marpaung, D. Rancang Bangun Mesin Giling Kopi Untuk Menunjang Dan Membuka Unit Usaha Baru Mitra Deli Coffe. *ABDI SABHA J. Pengabdi. Kpd. Masy.* **2022**, *3*, 174–180. [CrossRef]
16. Saberian, M.; Li, J.; Donnoli, A.; Bonderenko, E.; Oliva, P.; Gill, B.; Lockrey, S.; Siddique, R. Recycling of Spent Coffee Grounds in Construction Materials: A Review. *J. Clean. Prod.* **2021**, *289*, 125837. [CrossRef]
17. Atheba, P.; Allou, N.B.; Drogui, P.; Trokourey, A. Adsorption Kinetics and Thermodynamics Study of Butylparaben on Activated Carbon Coconut Based. *J. Encapsulation Adsorpt. Sci.* **2018**, *8*, 39–57. [CrossRef]
18. Moraes, L.E.Z.d.; Marcoti, F.A.O.; Lucio, M.A.N.; Rocha, B.C.d.S.; Rocha, L.B.; Romero, A.L.; Bona, E.; Peron, A.P.; Junior, O.V. Analysis and Simulation of Adsorption Efficiency of Herbicides Diuron and Linuron on Activated Carbon from Spent Coffee Beans. *Processes* **2024**, *12*, 1952. [CrossRef]
19. Yousef, R.; Qiblawey, H.; El-Naas, M.H. Evaluation of Activated Carbon Fiber Packed-Bed for the Treatment of Gas-to-Liquid Wastewater: Experimental, Modeling and ASPEN Adsorption Simulation. *Emergent Mater.* **2024**, *8*, 1591–1603. [CrossRef]
20. Rocha, S.A.F.d.; Rocha, B.C.d.S.; Moraes, L.E.Z.d.; Villaça, J.M.P.; Scapin, D.; Santo, D.E.; Gonzalez, R.d.S.; Junior, O.V.; Peron, A.P. Evaluation and Simulation of the Adsorption Capacity of Octocrylene Sunscreen on Commercial Carbon and Biochar from Spent Coffee Beans. *Processes* **2024**, *12*, 1249. [CrossRef]
21. Juela, D.M. Comparison of the Adsorption Capacity of Acetaminophen on Sugarcane Bagasse and Corn Cob by Dynamic Simulation. *Sustain. Environ. Res.* **2020**, *30*, 23. [CrossRef]

22. Bouillot, B.; Teychené, S.; Biscans, B. An Evaluation of Thermodynamic Models for the Prediction of Drug and Drug-like Molecule Solubility in Organic Solvents. *Fluid Phase Equilib.* **2011**, *309*, 36–52. [CrossRef]
23. Tavan, Y.; Hosseini, S.H.; Ahmadi, G.; Olazar, M. Mathematical Model and Energy Analysis of Ethane Dehydration in Two-Layer Packed-Bed Adsorption. *Particuology* **2019**, *47*, 33–40. [CrossRef]
24. Bueno, M.d.l.Á.B.-R.d.H.; Boluda-Botella, N.; Prats Rico, D. Removal of Emerging Pollutants in Water Treatment Plants: Adsorption of Methyl and Propylparaben onto Powdered Activated Carbon. *Adsorption* **2019**, *25*, 983–999. [CrossRef]
25. Anisuzzaman, S.M.; Bono, A.; Krishnaiah, D.; Tan, Y.Z. A Study on Dynamic Simulation of Phenol Adsorption in Activated Carbon Packed Bed Column. *J. King Saud Univ.-Eng. Sci.* **2016**, *28*, 47–55. [CrossRef]
26. Danaci, D.; Webley, P.A.; Petit, C. Guidelines for Techno-Economic Analysis of Adsorption Processes. *Front. Chem. Eng.* **2020**, *2*, 602430. [CrossRef]
27. USACE. *Design, Construction, and Operation Small Wastewater Systems*; EM 1110-2-501; USACE Publications-Engineer Manuals: Washington, DC, USA, 1999.
28. Rietveld, L.; Van Der Helm, A.; Van Schagen, K.; Van Der Aa, R.; Van Dijk, H. Integrated Simulation of Drinking Water Treatment. *J. Water Supply Res. Technol.-AQUA* **2008**, *57*, 133–141. [CrossRef]
29. Lakshmipathy, R.; Sarada, N.C. A Fixed Bed Column Study for the Removal of Pb^{2+} Ions by Watermelon Rind. *Environ. Sci. Water Res. Technol.* **2015**, *1*, 244–250. [CrossRef]
30. Inglezakis, V.J.; Balsamo, M.; Montagnaro, F. Liquid-Solid Mass Transfer in Adsorption Systems-An Overlooked Resistance? *Ind. Eng. Chem. Res.* **2020**, *59*, 22007–22016. [CrossRef]
31. Biswas, S.; Sharma, S.; Mukherjee, S.; Meikap, B.C.; Sen, T.K. Process Modelling and Optimization of a Novel Semifluidized Bed Adsorption Column Operation for Aqueous Phase Divalent Heavy Metal Ions Removal. *J. Water Process Eng.* **2020**, *37*, 101406. [CrossRef]
32. Zhang, Y.; Sivakumar, M.; Yang, S.; Enever, K.; Ramezanianpour, M. Application of Solar Energy in Water Treatment Processes: A Review. *Desalination* **2018**, *428*, 116–145. [CrossRef]
33. Luukkonen, T.; Pehkonen, S.O. Peracids in Water Treatment: A Critical Review. *Crit. Rev. Environ. Sci. Technol.* **2017**, *47*, 1–39. [CrossRef]
34. Teodosiu, C.; Gilca, A.F.; Barjoveanu, G.; Fiore, S. Emerging Pollutants Removal through Advanced Drinking Water Treatment: A Review on Processes and Environmental Performances Assessment. *J. Clean. Prod.* **2018**, *197*, 1210–1221. [CrossRef]
35. Crini, G.; Lichtfouse, E. Advantages and Disadvantages of Techniques Used for Wastewater Treatment. *Environ. Chem. Lett.* **2019**, *17*, 145–155. [CrossRef]
36. El-Sayed Abdel-Raouf, M.; Maysour, N.E.; Kamal Farag, R.; Mahmoud Abdul-Raheim, A.-R. Wastewater Treatment Methodologies, Review Article. *Int. J. Environ. Agric. Sci.* **2019**, *3*, 018.
37. Dhote, J.; Ingole, S.; Chavhan, A. Review on Wastewater Treatment Technologies. *Int. J. Eng. Res. Technol.* **2012**, *1*, 111–126.
38. Yoom, H.; Shin, J.; Ra, J.; Son, H.; Ryu, D.; Kim, C.; Lee, Y. Transformation of Methylparaben during Water Chlorination: Effects of Bromide and Dissolved Organic Matter on Reaction Kinetics and Transformation Pathways. *Sci. Total Environ.* **2018**, *634*, 677–686. [CrossRef] [PubMed]
39. Mao, Q.; Ji, F.; Wang, W.; Wang, Q.; Hu, Z.; Yuan, S. Chlorination of Parabens: Reaction Kinetics and Transformation Product Identification. *Environ. Sci. Pollut. Res.* **2016**, *23*, 23081–23091. [CrossRef] [PubMed]
40. López-Timoner, R.; Duarte-Alvarado, V.; Castillo, M.Á.; Santos-Juanes, L.; Arques, A.; Amat, A.M. Parabens and Methylisotiazolinone (MIT): Preservatives with Different Behaviors When Subjected to Ozone and Ultraviolet Light Treatments. *Water* **2023**, *15*, 3837. [CrossRef]
41. Simate, G.S.; Ndlovu, S. The Removal of Heavy Metals in a Packed Bed Column Using Immobilized Cassava Peel Waste Biomass. *J. Ind. Eng. Chem.* **2015**, *21*, 635–643. [CrossRef]
42. Soriano, A.N.; Orfiana, O.N.; Pangon, M.B.J.; Nieva, A.D.; Adornado, A.P. Simulated Biosorption of Cd(II) and Cu(II) in Single and Binary Metal Systems by Water Hyacinth (*Eichhornia crassipes*) Using Aspen Adsorption®. *ASEAN J. Chem. Eng.* **2016**, *16*, 21–43. [CrossRef]

Disclaimer/Publisher's Note: The statements, opinions and data contained in all publications are solely those of the individual author(s) and contributor(s) and not of MDPI and/or the editor(s). MDPI and/or the editor(s) disclaim responsibility for any injury to people or property resulting from any ideas, methods, instructions or products referred to in the content.